

UNCLASSIFIED

AD 267 977

*Reproduced
by the*

ARMED SERVICES TECHNICAL INFORMATION AGENCY
ARLINGTON HALL STATION
ARLINGTON 12, VIRGINIA



UNCLASSIFIED

NOTICE: When government or other drawings, specifications or other data are used for any purpose other than in connection with a definitely related government procurement operation, the U. S. Government thereby incurs no responsibility, nor any obligation whatsoever; and the fact that the Government may have formulated, furnished, or in any way supplied the said drawings, specifications, or other data is not to be regarded by implication or otherwise as in any manner licensing the holder or any other person or corporation, or conveying any rights or permission to manufacture, use or sell any patented invention that may in any way be related thereto.

CATALOGUED BY ASTIA
AS AD NO. 267977

Investigation of the Conduction Mechanism in

Insulating Solids

Contractor: Walter Eric Spear, University of Leicester,
Leicester, England.

Contract: DA - 91 - 591 - EUC - 1614

Report: Final Technical Report No. 2 November 1961.

Period: 1st November, 1960 - 30th November, 1961

The research reported in this document has been made possible through the support and sponsorship of the U.S. Department of Army, through its European Research Office.

62-14
XEROX

ASTIA AVAILABILITY NOTICE
QUALIFIED REQUESTORS MAY OBTAIN COPIES
OF THIS REPORT FROM ASTIA

513600
ASTIA
DEC 15 1961
JIPOR

Summary

This report describes further work on the charge transport in insulating solids. As in the earlier experiments, (F.T.R.1.), fast pulse methods have been used to study the drift mobility of generated carriers. In part A of the report a number of improvements in the experimental method are described. For measurements involving transit times of 40 nsec or less it was found essential to shorten the duration of the excitation pulses. Details of an electron pulse generator are given which provides pulse length from 5 to 500 nsec with rise times of less than 1 nsec. A further improvement is the use of a compact low capacity gating unit which employs a polarised mercury wetted switch. Field pulses of up to 1800 V can now be applied to the specimen without affecting the amplifier performance. Another application of a mercury relay is the field pulse generator producing fast rising voltage pulses of up to ± 1800 V. Finally a miniature optical lever arrangement is described which was found useful for the measurement of crystal thickness between the electrodes.

Part B deals with the investigation of carrier mobility and charge transport in monoclinic Se crystals which consist of a lattice of puckered Se_8 rings. As similar experiments have been carried out on the vitreous form (chain molecules) a comparison of the charge transport in these two structures can be made. Monoclinic crystals were grown from solution by a circulation method which is briefly described. At room temperature the electron mobility was found to be $2 \text{ cm}^2 \text{V}^{-1} \text{sec}^{-1}$. At temperatures above 0°C , $\mu \propto T^{-3/2}$ for all specimens. With decreasing T a sharp transition takes place from the lattice mobility to a charge transport controlled by a level of states $\epsilon = 0.25$ eV below the conduction band. A comparison of experimental and calculated μ vs. T. curves leads to a density of centres of about 10^{14} cm^{-3} . The same value of ϵ was found in experiments on vitreous Se suggesting that this type of centre is common to both forms. The hole mobility in monoclinic Se is found to be trap controlled throughout the temperature range investigated.

In part C the recent work on CdS crystals is discussed. A series of initial experiments have been carried out to investigate the effect of

various electrode materials on the response to the fast excitation pulses. It appears that for the observation of carrier transits, the free carriers must be generated near a blocking electrode, but the opposite electrode should be injecting. Room temperature measurements carried out on specimens with Au (top) and In (bottom) electrodes led to $\mu = 280 \text{ cm}^2 \text{V}^{-1} \text{sec}^{-1}$ for the electron drift mobility in good agreement with Hall mobility values. With decreasing temperature μ goes through a maximum and then decreases exponentially. Using crystals with exceptionally long hole life times, it has been possible to measure the drift mobility of holes in CdS. μ_h is about $0.2 \text{ cm}^2 \text{V}^{-1} \text{sec}^{-1}$ at room temperature. With increasing temperature μ_h appears to be closely proportional to $T^{-3/2}$.

Index

	<u>Page</u>
Summary	1
Index	3
<u>Part A: Improvements in the Experimental Method.</u>	
1. Introduction	4
2. Design of nsec Electron Pulse Generator	5
3. Specimen Holder and Amplifying System	8
4. Gating unit	9
5. Production of Field Pulses	10
6. Thickness Measurement of CdS Crystal Specimens	11
<u>Part B: Carrier Mobility and Charge Transport in Monoclinic Se crystals.</u>	
1. Introduction	12
2. Specimen Preparation	13
3. Experimental Procedure and Results	15
4. Discussion	19
<u>Part C: Carrier Mobility in CdS Crystals.</u>	
1. Introduction	22
2. Electron Mobility Measurements	22
3. Hole Mobility	27
References	29
Administrative Details	29

A. Improvements in the Experimental Method.

1. Introduction.

As the principle of the experimental method used in this investigation has been described previously in some detail^{1,2} only a brief outline of the method will be given here.

A fast pulse of electrons having energies up to 40 kev enters the top electrode of the specimen under investigation and generates electron-hole pairs to within a depth of a few microns below the top electrode. About 2 msec before the arrival of the excitation pulse a pulsed electric field is applied across the specimen for a few milliseconds and, depending on its polarity, either electrons or holes are drawn out of the surface region and drift across the specimen. The charge displacement is integrated and displayed on wide band electronic equipment.

In most of the experiments described in parts B and C the transit time of the carriers has been measured as a function of the applied field leading to a value for the drift mobility. This is generally studied as a function of temperature and has led to interesting conclusions about the nature and mechanism of the carrier transport. In some experiments¹ the number of charge carriers crossing the specimen has been investigated as a function of the applied field and the number and energy of the incident electrons. Such experiments can give information on the recombination process in the excited volume and allow an estimate to be made of the average energy required to generate an electron-hole pair by fast electrons.

For the interpretation of the experimental results and for the observation of well defined transit times it is essential to prevent the gradual build-up of an internal space charge which is likely to lead to a highly non-uniform internal field. Such effects are most likely connected with the gradual filling up of deeper trapping centres possessing thermal release times for longer than the time between excitation pulses.

The most effective precaution to reducing the effects of deep trapping consists in keeping the number of generated carriers per pulse as low as

is compatible with the sensitivity of the amplifying equipment. A second important precaution lies in the use of a pulsed applied field. This appears to reduce considerably the injection of additional carriers from the electrodes which, under steady field conditions, would lead to a far higher occupation of the deep centres.

2. Design of nsec Electron Pulse Generator.

The experimental determination of the carrier mobilities is based on the assumption that the excitation pulse is of much shorter duration than the transit time. As the work described in this report involved transit times as low as 40 nsec a considerable improvement in the performance of the electron pulse generator seemed essential.

Figure 1a shows the new unit³. It consists essentially of the tetrode electron gun G which is modulated by a fast voltage pulse generator. The latter employs the well known technique in which an open ended delay line DL is discharged by a fast switching device. For this, and the applications described in section 4 and 5, mercury wetted contact relays⁴ have been found very suitable. Although their application is limited to cases in which low repetition rates and fluctuations in the time interval between successive operations can be tolerated, the attraction of these relays lies in their comparative simplicity and in the ease with which extremely fast rising pulses can be obtained.

As shown in figure 1a the voltage pulse generator is constructed from two pieces of brass tubing (0.375" I.D.), hard soldered together to form a T-piece. The vertical part houses the polarised mercury switch capsule MS and carries at its upper end a 75 Ω type BNC socket for connection to the relay line. The horizontal tube carries two BNC pulse output sockets. Selected $\frac{1}{2}$ W composite carbon resistors (25 Ω) are incorporated in each section of the inner conductor (0.110") to give the correct output impedance. The dimensions have been chosen to provide as far as possible a 75 Ω match throughout the generator.

The normally open relay contact carries a small steel socket H which, together with the permanent magnet M, provides the necessary polarisation

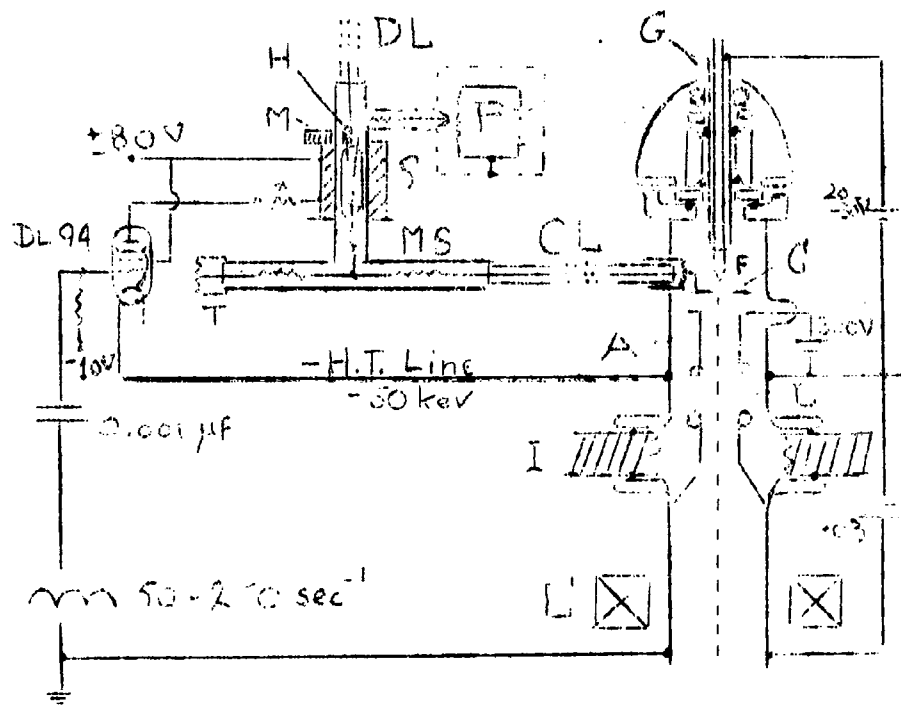


Figure 1 a.
msec Electron Pulse Generator

MS - Mercury switch capsule; DL - delay line; CL - Connecting line; M - polarising magnet; H - steel socket; P - potentiometer; S - solenoid; T - terminating socket; F - hairpin filament; G - glass tube; C - control grid; A - accelerating electrode; L - electrostatic lens; L' - magnetic lens; I - insulation.

(see also figure 2). The switching solenoid S consists of 5000 turns of 38 S.W.G. wire and requires an operating current of 3 - 4 m.a. The delay line is charged to the required potential through the 50 K Ω resistor mounted in a screened side tube close to the delay line socket. For the normal type of co-axial cable with polyethylene insulation ($\epsilon = 2.3$), the duration of the voltage pulse is very nearly 10 nsec for each metre of open ended delay line.

The inner conductor of the connecting line GL enters the demountable electron gun through a glass-metal seal close to the control grid aperture G. The line is terminated at the aperture by a 75 Ω carbon resistor. The hairpin filament F is spot welded to tungsten supports sealed into the glass tube G. O-ring seals allow both lateral and vertical adjustment of the filament with respect to the grid aperture under running conditions. The emission is biased off by a positive potential of 20-30V applied to F. The magnitude of the beam current which flows for the duration of the positive pulse is controlled by the potentiometer P. Electrode A at + 300V makes the beam current practically independent of the main accelerating potential (5-50kV) which is applied across the electrostatic lens L.

As both the gun and the pulse generator are kept at high potential, the relay is switched through a coupling condenser and a small amplifier. The indicated voltage levels refer to the - H.T. line. A rectified sinusoidal voltage is applied to the earthy side of the condenser, which could be replaced with advantage by a simple peaking transformer, preferably with an electrostatic screen. The resulting electron pulses, displayed on a 500Mc/sec sampling oscilloscope possess a rise time of less than 1 nsec. The unit is normally run at a pulse repetition frequency of 50 or 100 sec^{-1} . A number of prepared delay lines provide pulse lengths from 5 to 500 nsec.

If an external trigger signal is required the following simple, but not altogether satisfactory, method has been used. A few turns of wire are connected in series with the termination T of the second pulse output. The signal is picked up at the low potential end and used as a trigger after amplification. However, the mismatch introduced by the inductive component leads to a deterioration of the electron pulse.

3. Specimen Holder and Amplifying System.

The modified specimen holder is shown in figure 1b. The electron beam, focussed to a circular spot of 2.5mm diameter enters the top electrode of the specimen S. The bottom electrode is connected to a cathode follower CF mounted close to it to reduce the input capacity as far as possible. By suitable choice of R the input time constant is made much longer than the transit time under investigation. During this time the potential across R is therefore proportional to the total charge displacement of the drifting carrier cloud. The output of the cathode follower is fed into two distributed pre-amplifiers connected in series (Hewlett-Packard, type 460 AR, bandwidth 120Mc/sec). A Tektronix 581 oscilloscope (bandwidth 100Mc/sec) is used to display the signal. The system possesses an overall rise time of about 5 nsec and with the normal specimen capacity 1cm of vertical deflection represents the transit of approximately 10^5 charge carriers. The charge sensitivity is determined by applying a calibration pulse to the input through the small standard condenser C_s .

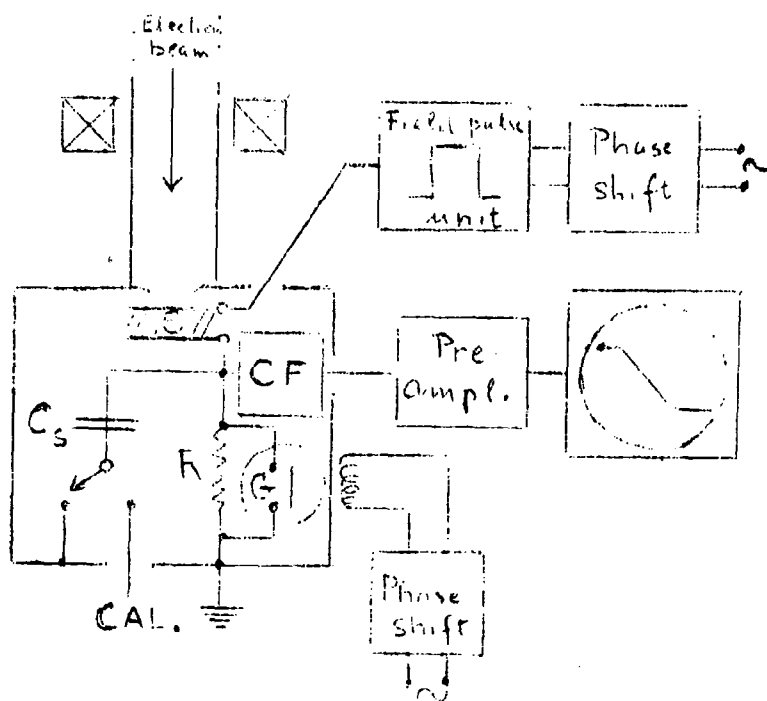


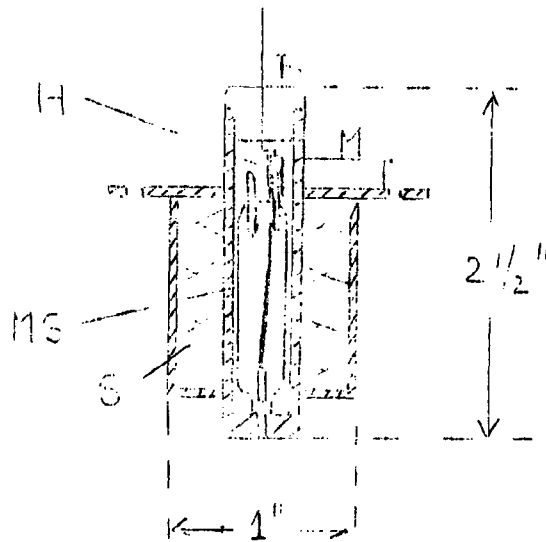
Figure 1 b

The top electrode of the specimen is connected to a pulse generator which provides field pulses of 4 msec duration at a repetition frequency of 50 sec^{-1} (section 5). The phase of the field pulse with respect to the electron excitation pulse can be adjusted by means of a phase shift network.

During the application and removal of the applied field the gating unit G (section 4) shorts out the resistor R to prevent paralysis of the amplifying system. Phase and duration of the open gate can be adjusted independently. Normally the gate opens 1 msec before the excitation pulse and closes 1 msec after it.

4. Gating Unit.

The mercury switch provides a simple and effective answer to the problem of input gating³. A compact unit used widely in the present work is shown in figure 2. With the relay in the 'open' position, the capacity of the unit is about 2pf and its effect on the input capacity is normally negligible



Figure

It should be noted that in this case the steel socket H and the polarising magnet M are placed on the side of the normally closed relay contact. With a rectified sinusoidal potential applied to the solenoid

the open gate could be varied between 1 msec and 5 msec by adjustment of the current or the magnet position.

It was found possible to apply voltage pulses of up to $\pm 1800V$ across the specimen without affecting the amplifier performance. The switching transients produced by the gate were found to be negligibly small even at maximum sensitivity. This may be partly due to the limited low frequency response of the amplifiers and the small specimen capacity.

5. Production of field pulses.

The field pulse generator described in F.T.R. 1 has been replaced by the much simpler unit shown schematically in figure 3. It employs an unpolarised mercury switch M which is energised from the A.C. mains through a phase shift network and a half- or full-wave rectifier R giving repetition frequencies of 50 or 100 sec^{-1} . The unit has been used for pulse heights up to $\pm 1800V$ with no sign of deterioration or damage to the relay. The voltage source has been built up of small size 90V and 300V layer type batteries. With a tapping point at 30V and 60V, the complete voltage range could be covered in 30V steps by the use of 3 selector switches.

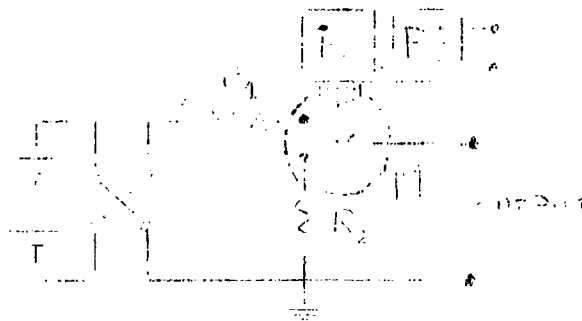


Figure 3

During switching the mercury droplet adheres to the armature and shorts out contacts 1 and 2 for a fraction of a msec. Resistors R_1 and R_2 are therefore necessary to limit the current flow from the voltage source. With $R_1 = 0$, $R_2 = 4.7 \text{ M}\Omega$ the pulse rises in a few nsec, but the falling edge has a time constant of about 70 μsec . Oscillations of small amplitude

tend to occur on top of the pulse near the rising edge. These are damped out with $R_1 = 1K$ which leads to a rise time of less than 15 nsec.

6. Thickness Measurement of CdS crystal Specimens.

As the mobility values calculated from the experimental data depend on the square of the distance between the electrodes it is essential to determine this quantity with reasonable accuracy. It was found difficult to do this particularly with small fragile crystals which were not necessarily plane parallel over the complete surface. The following simple method has been found extremely useful in connection with CdS crystals and is shown in figure 4. It consists of a miniature optical level which is easily

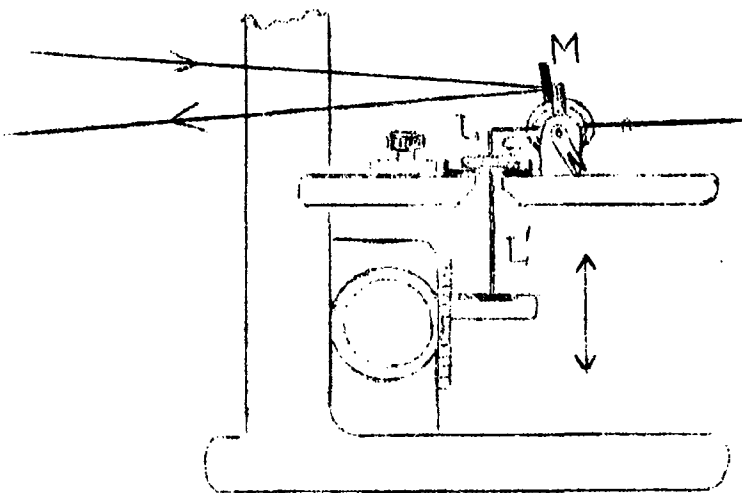


Figure 4

made from the well balanced moving coil system of a D.C. meter. A small mirror M is stuck to the moving coil, and reflects the image of a horizontal wire on to a scale at a distance of about 5 m. The vertical part of the lever, L , consists of a small steel needle carefully rounded off at its lower end. The arrangement is screwed on to the table of a microscope, and the microscope condenser is replaced by a similar needle L' . The crystal C rests on the slide traverser so that its position in a horizontal

plane can be adjusted with respect to L and L'. L is lowered on to the crystal, the coil spring of the meter movement applying a gentle pressure. L' is moved upwards until it touches the crystal, which occurs when the light spot begins to move from its initial position. The crystal is removed and the difference in reading gives the local thickness. In this way the electrode region is tested for uniformity and the average thickness over the bombarded region can be obtained. The system is calibrated with feeler gauges and possesses a sensitivity of about 1 μ per mm of scale deflection.

B. Carrier Mobility and Charge Transport in Monoclinic Se Crystals.

1. Introduction.

The study of the electrical properties of the Se allotropes allows a comparison between the charge transport in a chain and a ring structure of the same element. In contrast to the hexagonal and vitreous modifications the monoclinic form of Se consists of a lattice of puckered Se_8 rings^(5,6). An α and β monoclinic form have been distinguished but there appears to be little structural difference between them⁽⁷⁾. Photoconductivity in these crystals was first investigated by Gudden and Pohl⁽⁸⁾ and recently a detailed investigation of the optical properties has been carried out by Prosser⁽⁹⁾. Virtually nothing is known about the electrical properties of monoclinic Se.

The experimental method described in Part A of this report has been applied to a detailed investigation of the carrier mobility and the conduction mechanism in monoclinic Se crystals. Since similar experiments have been carried out on the vitreous form^(1,2) which consists of Se chain molecules, a comparison of the charge transport in the two forms can be made.

An interesting feature of the present experiments is the transition from the lattice mobility to a charge transport controlled by a level of discrete states. A similar behaviour has been observed by Brown and Kobayashi⁽¹⁰⁾ in AgCl crystals.

2. Specimen Preparation.

The growing of crystals of sufficient size and perfection presents one of the main problems. The circulating method originally used by Kyropoulos⁽¹¹⁾ was tried under various experimental conditions but the crystals were imperfect and too small. An improved method due to Prosser⁽⁹⁾ which is shown in figure 5 led to far better results.

The solvent, re-distilled CS_2 , is boiled in a flask fitted at its side with the water-cooled circulation tube C. The condensed vapour passes into a Soxhlet Extractor and drips through the filter funnel N filled with precipitated red Se powder. The saturated solution rises in the tube below F and eventually overflows into the flask. In this way the solvent is gradually saturated with Se and red monoclinic crystals begin to form in the lower part of the circulation tube. The advantage over the Kyropoulos method lies in the fact that the solvent remains completely free from small particles of Se powder which previously appeared to form nucleation centres and led to a large number of small crystals.

With this method up to 20 crystal plates 40-70 μ thick, and measuring 2½-3mm across, could normally be obtained in a run lasting about 20 hours. Various positions of the cooling jacket around the circulation tube were tried; the best batch of crystals was obtained when the cooling was confined to the vertical part of the circulation tube. An X-ray examination* of a number of crystals led to lattice parameters in close agreement with those of the β -monoclinic form. According to the structure determined by Burbank⁽⁶⁾ the (101) plane coincides with the surface of the crystal plates; the average planes containing the puckered Se rings are almost perpendicular to the surface. Microscopic examination showed pronounced surface steps and striations on many of the crystals. A number of specimens with little or no surface structure were selected and fitted with evaporated gold electrodes of 1-2mm² area on opposite sides of the crystal plate. Thin connecting wires were attached with silver paste. The specimen was mounted in a vacuum chamber designed for temperature measurements.

* carried out by Dr. M. Ehrenberg of University College, London.

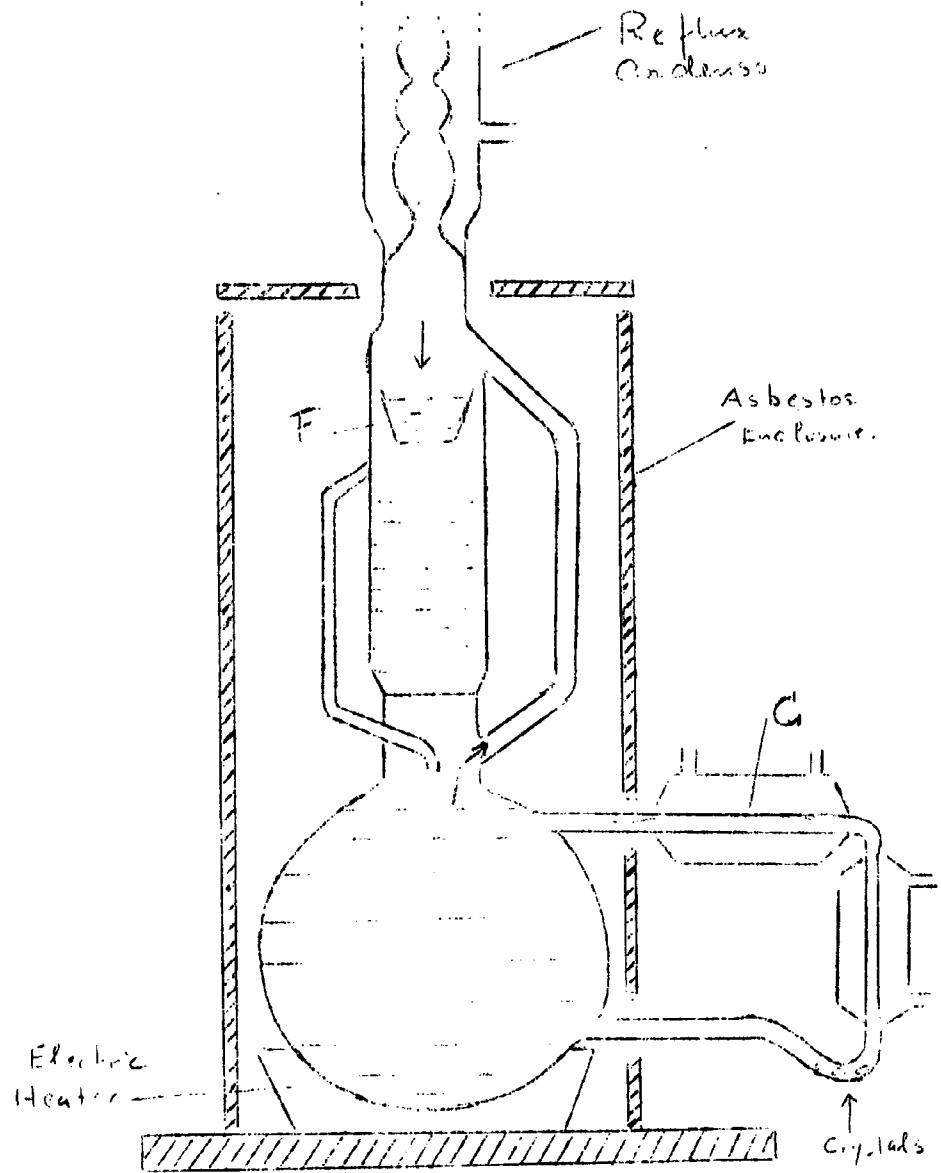


Figure 5
Method of Synthesis of Crystals

3. Experimental Procedure and Results.

Figure 6 shows a typical photograph of the oscilloscope trace when generated electrons are drawn across a monoclinic crystal in an applied field of $4.5 \times 10^4 \text{ v cm}^{-1}$ at room temperature. 40 kev excitation pulses of 8 nsec duration have been used. The average depth of the excited volume below the top electrode (about 5μ) is therefore small compared to the specimen thickness. The linear edge of the pulse implies a uniform drift velocity of the carriers indicating that a) the internal field is uniform, and b) the number of electrons per pulse leaving the recombination region near the top electrode remains constant during transit. The sharp levelling off of the trace marks the arrival of the generated electrons at the bottom electrode and defines a transit time t_t , in this case 60 nsec. The pulse height corresponds to the transit of less than 10^6 carriers produced at $t = 0$ by the incident pulse of 2.5×10^4 electrons (not resolved in figure 6).

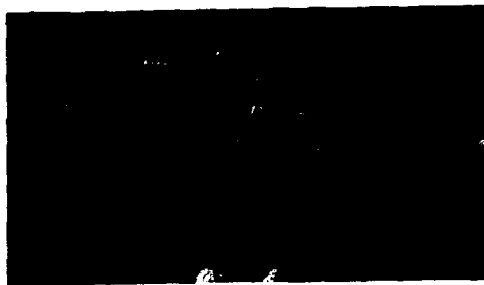


Figure 6.

The experimental procedure consisted in measuring t_t as a function of the applied field E which ranged from about 5×10^3 to $7 \times 10^4 \text{ v cm}^{-1}$. The graph of $1/t_t$ against E was found to ^{be} linear except for a small range of values at low applied fields. As explained previously⁽¹⁾ this is most likely due to space charge build-up in the surface region. A value for the mobility $\mu = d/Et_t$ where d denotes the specimen thickness, was obtained from the gradient of the graph.

The twelve specimens investigated were selected partly from a number of batches grown in this laboratory and partly from crystals supplied by

Dr. Prosser of Prague University. They all showed the same general behaviour. At room temperature the electron mobilities were found to lie between 1.7 and 2.3 $\text{cm}^2 \text{sec}^{-1} \text{v}^{-1}$. On a given specimen the values of t_t were reproducible to within a few per cent; the main error in μ arose from the difficulty of measuring the thickness of the fragile crystals (the method described in Part A, section 6, had not then been developed) to a comparable accuracy. In the following the mobilities have therefore been normalised to the value μ_r at room temperature T_r , to facilitate the correlation of results from different specimens.

The experimental points in figure 7 show the temperature dependence of μ/μ_r for three specimens typical of the crystals investigated. The continuous lines were calculated from equation (3) of section 4. Above 0°C the mobility of all the specimens was proportional to $T^{-3/2}$ which would be expected in a non-polar crystal from the interaction of the generated electrons with the lattice vibrations⁽¹²⁾. As the temperature is lowered, however, μ/μ_r goes through a maximum and then decreases sharply. In figure 8 the same experimental data have been plotted on a semi-logarithmic graph against $10^3/T$. It shows fairly convincingly that with decreasing temperature the mobility-temperature dependence goes over into a relation of the form $\mu \propto e^{-\epsilon/kT}$ with $\epsilon = 0.25\text{ev}$. It is of interest to compare these results with the electron mobility in the vitreous form^(1,2). As can be seen from figure 3 this shows an exponential dependence throughout the temperature range which is associated with practically the same value of ϵ .

At temperatures in the region of the mobility maximum and below it is observed that the levelling off of the pulse becomes less sharp than is shown in figure 6. The initial part of the pulse, however, retains its linearity and the more gradual rounding off affects at most the final 30% of the pulse length. It appears, therefore, that the generated electron cloud spreads out during transit. As diffusion is an unlikely explanation this straggling in the arrival times is almost certainly connected with trapping in a level of centres with release times which are short, but not negligibly so, in comparison with t_t . The mechanism

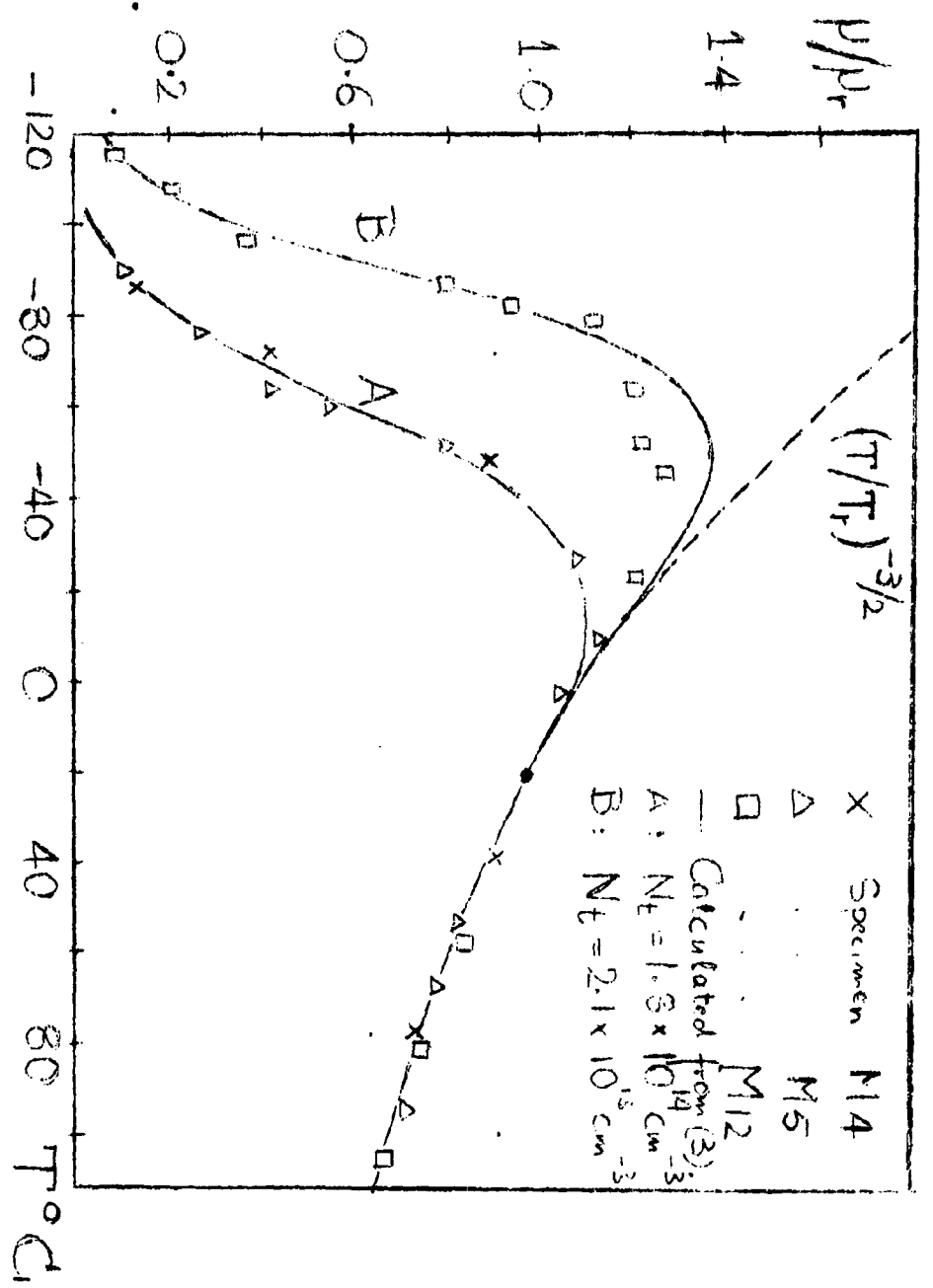


Figure 7.
Temperature Dependence of μ/μ_r .

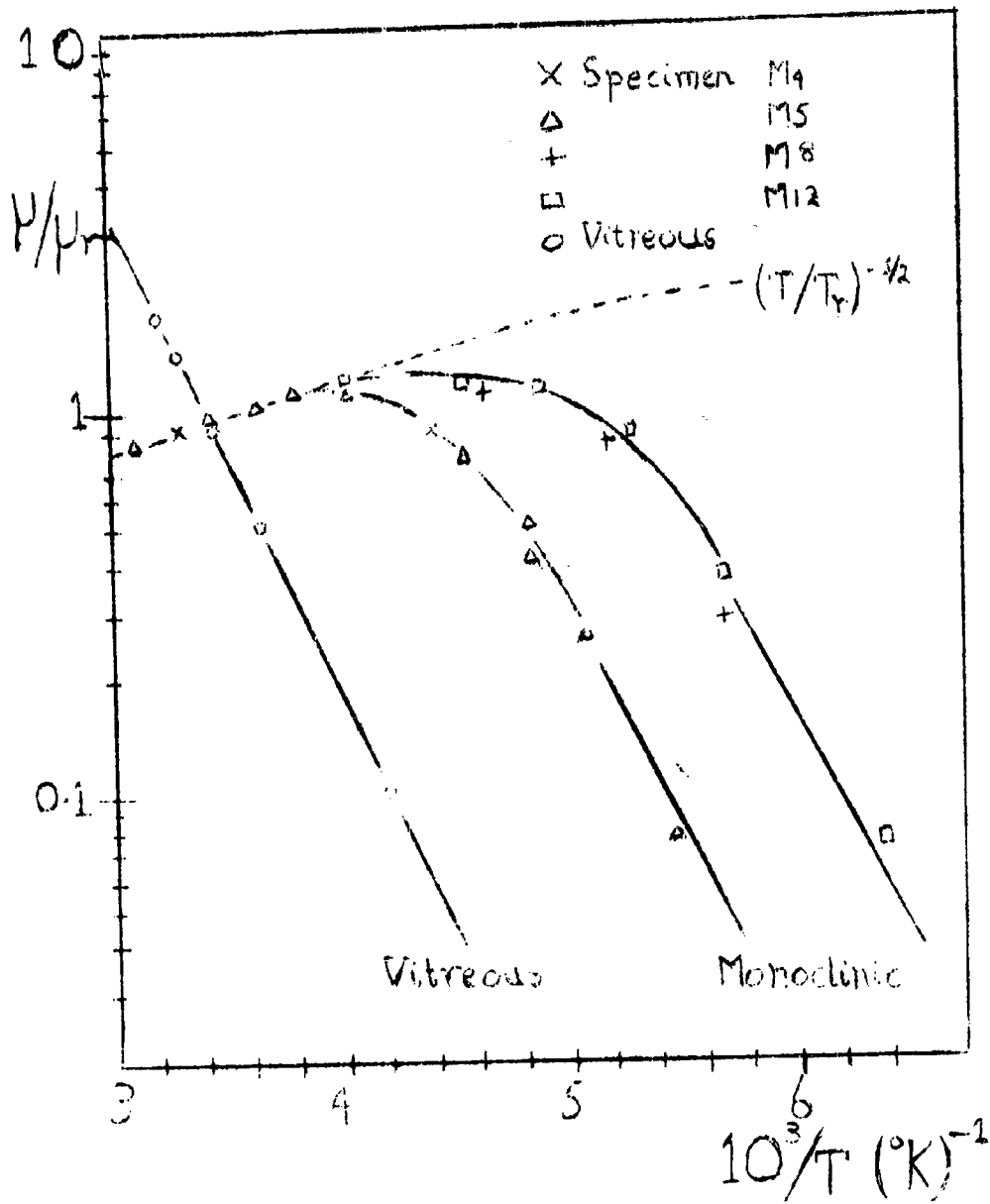


Figure 3

of trap controlled charge transport will be discussed further in section 4. In presence of the straggling of transit times it appeared reasonable to use an average value of t_t defined by the point of intersection of the linear portion with the final horizontal level.

The charge gain, i.e. the number of electrons drawn out of the surface region per incident electron, has been determined for a number of specimens at $E = 3 \times 10^4 \text{ v cm}^{-1}$ and is found to be about 40. It is about $\frac{1}{3}$ of that observed for vitreous specimens under identical conditions.

When the field across the specimen is reversed a positive signal is observed corresponding to the drift of generated holes. This has been investigated for a number of specimens with the following results:

- a) At room temperature and below there exists a marked difference in the height of the electron and hole signals. For example, at room temperature and $E \sim 10^4 \text{ v cm}^{-1}$ the positive signal is only $1/5$ of the electron amplitude and increases to about $\frac{1}{2}$ at maximum E . This fact, together with the observed pulse shape, indicates that deep trapping occurs during transit. Above 50°C , however, the ratio of the amplitudes approaches unity at the higher fields and the pulse possesses a linear edge as in the case of electrons. Transit time measurements could be carried out in this temperature range.
- b) The measured hole mobility increases with T up to the highest temperatures used. At 105°C $\mu_h = 1.3 \text{ cm}^2 \text{ v}^{-1} \text{ sec}^{-1}$; it is then nearly equal to the lattice controlled electron mobility at that temperature. Because of the limited temperature range that could be investigated, these results are less conclusive than those for the electron mobility. Above 50°C the experimental values could be fitted approximately to a relation of the form $\mu_h \propto e^{-\epsilon/kT}$ with $\epsilon \sim 0.3 \text{ ev}$.

4. Discussion.

The rapid decrease of the electron mobility shown in figure 7 is of interest because it suggests a change in the mechanism of charge transport. Normally the decrease in carrier mobility at low temperatures is connected with the transition from lattice to impurity scattering⁽¹³⁾. The latter

varies approximately as $T^{3/2}$ and leads to a far shallower mobility maximum. (14)
 Impurity scattering can obviously not explain the rapid decrease of μ
 within a comparatively small temperature range. The experimental
 temperature dependence at lower T suggests that the observations are
 connected with the transition from a mobility determined by lattice
 scattering to one controlled by a fairly narrow level of states of density N_t ,

ϵ ev below the conduction band. With decreasing temperature the mean
 free path between lattice scattering increases, and in the region of the
 mobility maximum becomes comparable with that between trapping events.
 This transition may be formulated in the following simple way if it is
 assumed that the effective drift velocity of the electron cloud is small
 enough to allow a description in terms of the equilibrium distribution
 between free and trapped carriers.

The measured mobility is given by

$$\mu = \frac{d}{(t_0 + \sum t_e) E} \quad (1)$$

where t_0 denotes the transit time in absence of trapping; this is
 determined by the lattice mobility $\mu_0 = d/Et_0$. t_e , the average time
 an electron remains in the level at ϵ is obtained by equating the rate
 of thermal release with the rate of trapping. This leads to $t_e = \tau (n_t/n_0)$
 where $n_t (\ll N_t)$ denotes the density of trapped electrons and τ the free
 electron lifetime. As the average number of trapping events during transit
 time is t_0/τ , $\sum t_e = t_0 (n_t/n_0)$. If the Fermi level lies
 below ϵ by more than a few kT ,

$$\sum t_e = \frac{N_t}{N_c} t_0 e^{\epsilon/kT} \quad (2)$$

The effective density of states is $N_c = 2.5 \times 10^{15} (T/T_r)^{3/2} (m^*/m)^{3/2}$.

Equation (1) and (2) together with $\mu_0/\mu_r = (T/T_r)^{-3/2}$ then lead to

$$\mu/\mu_r = \left[(T/T_r)^{3/2} + 0.4 \times 10^{-19} N_t (m^*/m)^{-3/2} e^{\epsilon/kT} \right]^{-1} \dots (3)$$

Using the value $\epsilon = 0.25$ ev obtained from figure 8, $N_t (m^*/m)^{-3/2}$

can be found from the position of the mobility maximum in figure 7.

For specimens M4 and M5, $N_t = 3.5 \times 10^{13} (m^*/m)^{-3/2} \text{ cm}^{-3}$, for M12

it is $4 \times 10^{12} (m^*/m)^{3/2} \text{ cm}^{-3}$. Other specimens lead to values within this range. It can be seen from figure 7 that with these constants equation (3) leads to a satisfactory agreement with experiment over the complete temperature range.

Moss⁽¹⁵⁾ has applied the deformation potential theory⁽¹²⁾ to obtain an estimate of the lattice mobility in Se. He finds $\mu (m^*/m)^{5/2} \approx 32$ at room temperature which leads to $m^* \approx 3m$, in reasonable agreement with the value $2.5m$ obtained from the Faraday effect.⁽¹⁵⁾ This may well be fortuitous in view of the uncertainty of the data used for the estimate of the deformation potential. With the above value of m^* , the specimens lead to an average value of 10^{14} cm^{-3} for N_t .

At a low temperature in the trap controlled range (e.g. -80°C , specimen M5) a transit time of about 300 n sec is observed at a normal value of E . From the extent of the straggling of transit times ($\approx 90 \text{ nsec}$), t_t might be estimated as 30 n sec. τ_0 which is given by $(N_t/\mu_e)t_t$ would then be about 3 n sec. With $N_t = 10^{14} \text{ cm}^{-3}$ this leads to a capture cross section of the order of 10^{13} cm^2 . One would expect such a comparatively high value to be associated with charged centres which exert a Coulomb attraction on the free electrons.

It is not possible at present to decide whether the centres arise from impurities or from structural defects. The close agreement in the value of ϵ for monoclinic and vitreous Se suggests that the type of centre controlling the electron mobility is common to both forms. A comparison of the measured mobility values indicates that N_t should be about 10^{18} cm^{-3} in the vitreous form. With a density of this order the transition to a lattice mobility would be expected only at temperatures well above the melting point.

It has been pointed out that the investigation of the hole mobility was complicated by the presence of deeper trapping effects; an interpretation of the results in terms of a single level at $E = 0.3 \text{ eV}$ is therefore doubtful. As would be expected there appears to be no connection between the hole mobility in the monoclinic and the vitreous (or hexagonal) forms. In the latter $\epsilon = 0.14 \text{ eV}$, a value which is characteristic of the hole transport along a Se chain.

Part C. Carrier Mobility in CdS Crystals

1. Introduction.

In view of the considerable interest shown in recent years in the properties of CdS it is surprising to find that comparatively little systematic work on the more fundamental aspects of the charge transport in these crystals is available. Kröger et al⁽¹⁶⁾ have studied the Hall Mobility of electrons between 20°K and 700°K by combining measurements made on pure and doped crystals. They concluded that in the range between 100°K and 700°K the temperature dependence of mobility is predominantly determined by lattice scattering. The results were interpreted in terms of the combined effects of a) non-polar scattering by acoustic modes, $\mu_n = b T^{-3/2}$, and b) polar scattering by longitudinal optical modes. A reasonable fit to the experimental data above about 200°K could be obtained using values of the Debye temperature between 250 and 300°K, of 'b' between 3.1×10^6 and 7.6×10^6 cm² degree^{3/2} volt sec., and effective mass ratios between 0.2 and 0.27.

On the other hand the results of Hall Mobility measurements obtained more recently by Piper and Halstead⁽¹⁷⁾ appear to be significantly different from the previous work. The temperature dependence of μ has been interpreted here in terms of the polar interaction with the optical modes alone using a value of 440°K for the Debye temperature which is more in agreement with independent measurements⁽¹⁸⁾. However, the fit of the theoretical curve in the higher temperature range, above 300°K, is unsatisfactory.

In view of these discrepancies it is of considerable interest to investigate the electron mobility in CdS by a different and more direct method than that based on a combination of Hall effect and conductivity measurements.

2. Electron Mobility Measurements.

The preliminary experiments, briefly described in F.T.R.1., showed clearly that the study of charge transport in CdS using fast pulse methods is complicated by secondary effects such as the injection of excess carriers from the electrodes. It was apparent that the choice of a suitable

electrode material was far more critical than with the other crystals previously investigated. In an attempt to solve this problem a series of initial experiments on the transient behaviour of several electrodes on CdS has been carried out.

A number of 'pure' (i.e. undoped) crystal plates (kindly supplied by Dr. J. Franks of A.E.I. Harlow) were fitted on both sides with evaporated In, Te and Au electrodes. Crystal thicknesses ranged between 50 and 250 μ . In addition specimens with a blocking top electrode and an In bottom electrode (denoted by B.E. - In) were prepared; the blocking electrode consisted of a thin piece of cleaved mica ($\sim 2 \mu$ thick) carrying an evaporated Au electrode. The uncoated side was gently pressed against the crystal surface.

The response to fast excitation pulses (5-100 nsec) using 4 msec field pulses as described in Part A, may be summarised as follows:-

In electrodes: No response to the fast pulses. Strong injection seems to obscure the transit of volume generated carriers.

Te electrodes: A fast component, followed by a slower charge displacement which lasts for about $\frac{1}{2}$ μ sec. The rise of the fast component did not appear to be directly connected with the transit of electrons across the specimen.

Au electrodes: No detectable response. Evaporated Au electrodes appear to be blocking, although after heating the crystal to about 300°C they become permanently injecting. It is possible that with blocking electrodes on both sides of the crystal a strong positive space charge will develop in the excited volume near the top electrode which would tend to annul the applied field throughout most of the specimen.

B.E. - In (B.E. negative): Well defined transit of generated electrons is observed using 5 nsec excitation pulses.

Au - In (Au negative): The above results suggest the use of an Au electrode instead of the mica blocking electrode; this was tried and again a well defined electron transit was observed.

To summarise, the following experimental conditions appear to be essential for the study of drift mobility in CdS:

- a) free carriers must be generated near a blocking electrode
- b) the opposite electrode must be injecting
- c) the applied field must be pulsed; no signal is observed with a steady field.

The conditions seem to ensure that when the field is switched off the remaining positive space charge is neutralised by injection through the In electrode before the arrival of the next excitation pulse.

A number of room temperature measurements of the electron mobility have been carried out on different crystals using both B.E.-In and Au-In electrodes. Figure 9 shows a typical graph of $1/t_t$ vs. applied voltage which allows the correlation of a number of transit time measurements over a range of values of V . The reproducibility of the points for a given specimen is good; the mobility values obtained for several different crystals lie between 240 and $290 \text{ cm}^2 \text{ V}^{-1} \text{ sec}^{-1}$ with a mean value of $280 \text{ cm}^2 \text{ V}^{-1} \text{ sec}^{-1}$. This is in good agreement with the Hall mobility value of Piper and Halstead,⁽¹⁷⁾ It compares equally well with the result of a new experiment recently carried out by Hutson et al.⁽²¹⁾ in which a drift mobility of $285 \text{ cm}^2 \text{ V}^{-1} \text{ sec}^{-1}$ has been deduced from the interaction of the drifting electron with an acoustic wave propagated through the crystal. The lower values of μ quoted previously in Q.T.S.R. No.6. (August 1961) were due to the inaccurate measurement of local thickness. Re-measuring these crystals with the optical lever device led to values within the above range.

So far a temperature run in the somewhat limited range from 100°K to 500°K has been carried out on one specimen. The results, which however require further confirmation, are shown in figure 10. Above room temperature, the mobility decreases rapidly as a result of increasing lattice scattering. At about 230°K the drift mobility, normalised in figure 10 to the room temperature values, goes through a maximum and then decreases exponentially. On the assumption that the model of a trap controlled mobility used in Part B is applicable in this case, the values of $E \approx 0.048 \text{ eV}$ and $N_t \approx 3 \times 10^{17} \text{ cm}^{-3}$ have been derived. It is possible that this level may be identified with the donor states found by both Kroger et al.⁽¹⁶⁾ and Piper and Halstead.⁽¹⁷⁾ At infinite dilution the latter estimate a donor binding energy of 0.032 eV . However, from their published curves of $\log R_H$ vs. $10^3/T$ it appears that the binding energy is about 0.015 eV for a donor concentration of $2 \times 10^{17} \text{ cm}^{-3}$ which lends some support to the above interpretation.

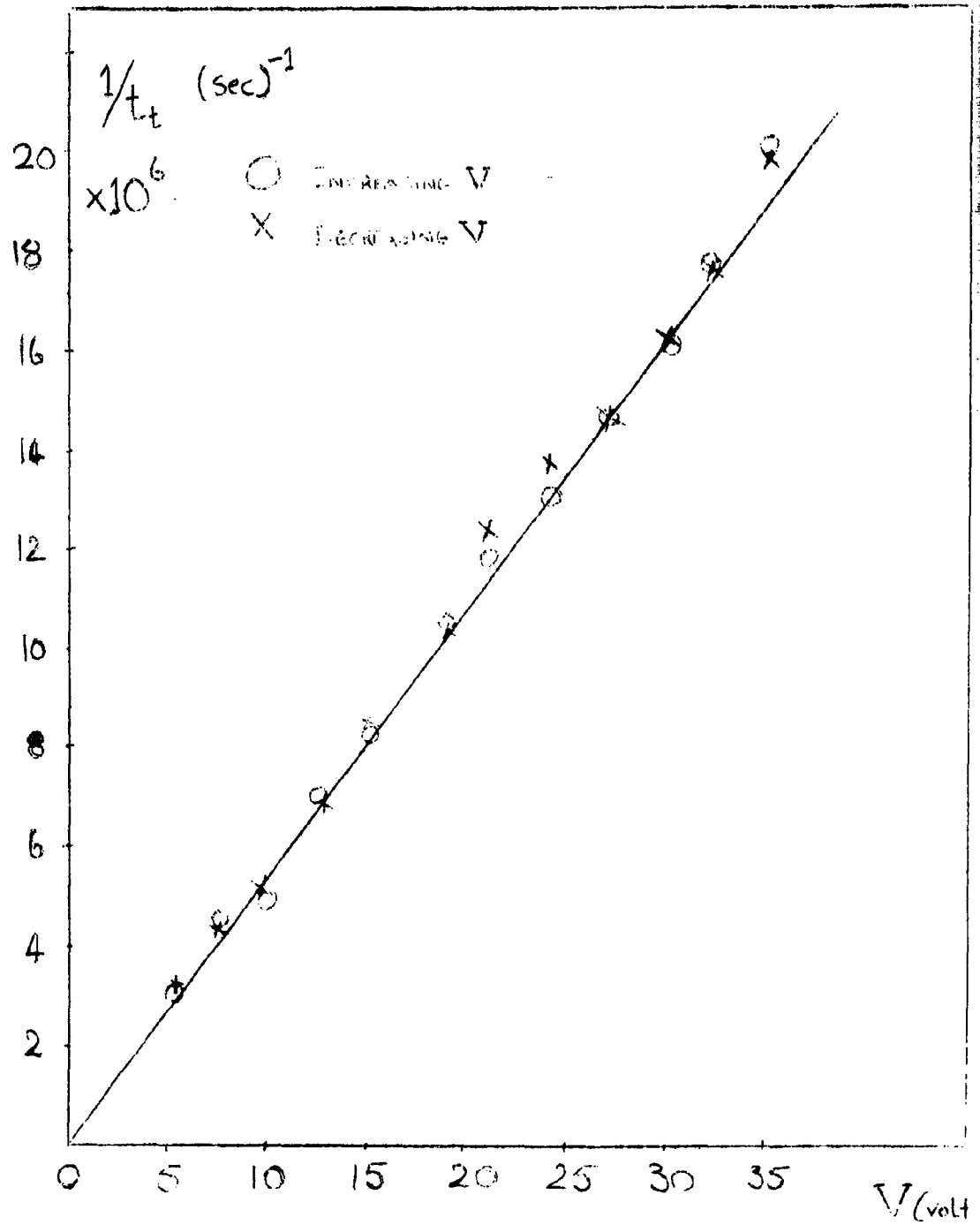


Figure 9

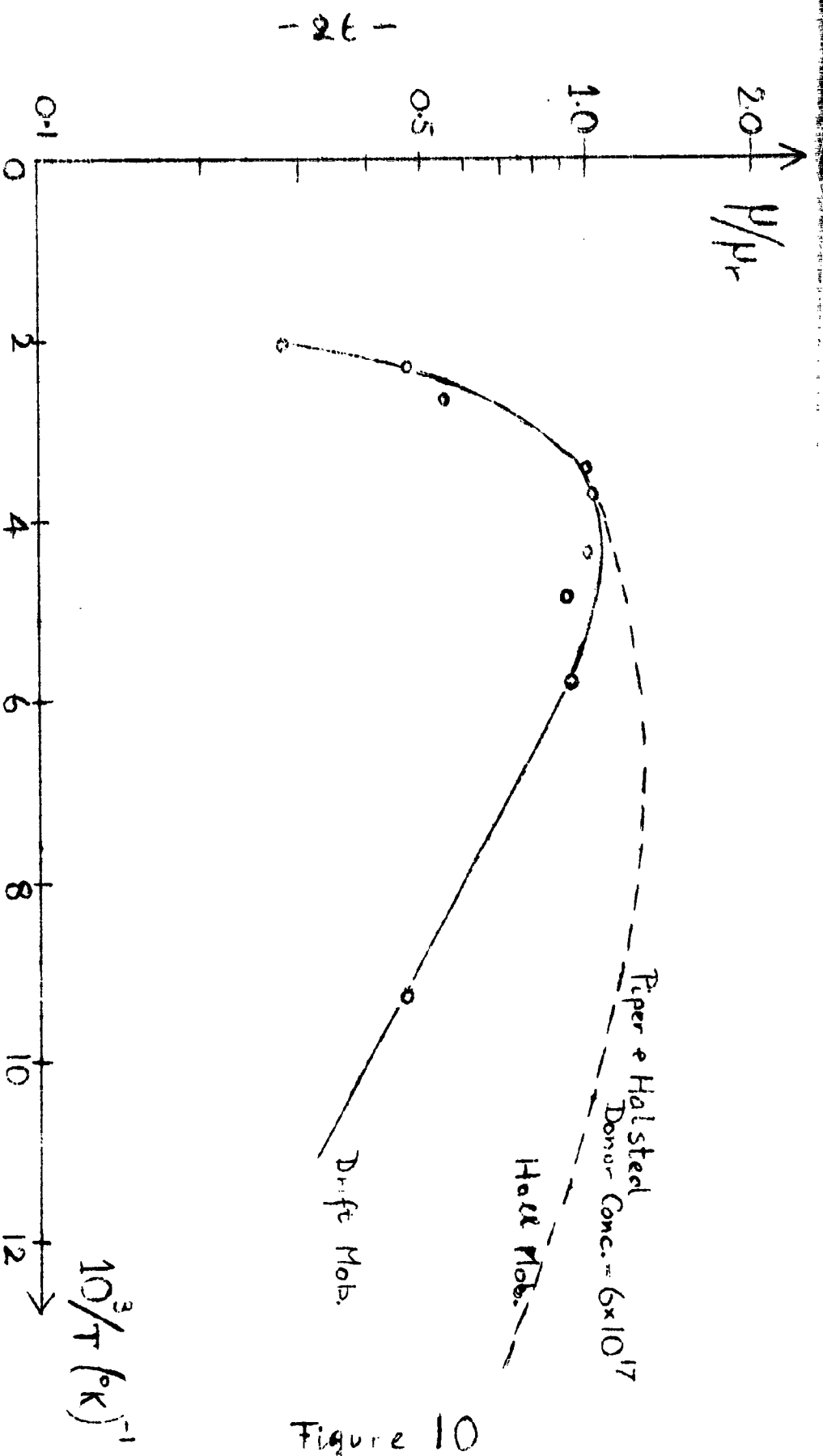


Figure 10

dependence

Figure 10 also shows the temperature of the Hall mobility as determined by Piper and Halstead for a donor concentration of $6 \times 10^{17} \text{ cm}^{-3}$. This is appreciably different, which would be expected if the above interpretation were correct. For a closer understanding of the mechanisms involved it would be of considerable interest to measure both drift and Hall mobility on the same specimen over a wider range of temperatures. A specimen holder suitable for the study of the electron-bombardment induced Hall effect is being constructed at present. In addition the measurements will be extended into the liquid hydrogen range.

3. Hole Mobility.

The question as to what extent holes are mobile in CdS has been a controversial one for some years. Van Heerden⁽¹⁹⁾ studied the primary photocurrent in CdS crystals under α -particle bombardment and found that his results were consistent with the presence of a primary hole current. However, the results suggested that the life time of holes in these crystals was extremely short, 10^{-11} sec or less.

In an investigation of the luminescence in CdS, Smith observed in a few crystals a green electroluminescence throughout the volume at fields as low as 1000 V/cm. The maximum spectral response coincided with the absorption edge and therefore appeared to be due to the recombination of free electrons and holes. Smith concluded that for these electroluminescent crystals the hole life time may be as long as 10^{-6} sec. Under these conditions hole transits should easily be observable with our apparatus. We are indebted to Dr. R.W. Smith of the R.C.A. Laboratories Princeton, N.J. for supplying us with a number of these crystals.

Preliminary measurements on two specimens showed indeed a well defined hole transit. The experiments are complicated by the small size of the crystals. In accordance with the general conclusions of section 2, the crystals were fitted with an In top electrode, assumed to be blocking for holes, and a Au bottom electrode. At room temperature the hole mobilities for the two crystals were about $0.2 \text{ cm}^2 \text{ V}^{-1} \text{ sec}^{-1}$.

Experiments on the temperature dependence of the hole mobility are being carried out at present. The first few runs at temperatures above room temperature show that μ_h steadily decreases with increasing T and that $\mu_h \propto T^{-3/2}$ very nearly. It appears therefore that non-polar scattering predominates in this temperature range, but more results are necessary before any definite conclusions can be drawn.

References

1. Spear, W.E., Final Technical Report No.1, October 1960, Contract DA-91-591-EUC-1269. Referred to as F.T.R.1. in the following.
2. Spear, W.E. 1960, Proc. Phys. Soc, 76, 826.
3. Spear, W.E., Lanyon, H.F.D., Mort J., 1961, Journ Sci. Instr. (in print)
4. Brown, J.T.L., Pollard, C.F., 1947, Electrical Eng. 66, 1106.
5. Klug, H.P., Z. Krist. 88, 108 (1934)
6. Burbank, R.D., Acta Cryst. 1, 140 (1951)
7. Marsh, E., Pauling L., and McCullough J.D., Acta Cryst. 6, 71 (1953)
8. Cudden, B., and Pohl, R., Z. Phys. 35, 243, (1925)
9. Prosser, V., Cs Jaz, Fys, A10, 35 (1960); Proceeding of the International Conference on Semiconductor Physics (1960), p.993.
10. Brown, F.C., and Iobayashi K., J. Phys. Chem. Solids 8, 300 (1959)
11. Kyropoulos S., Z. Phys. 40, 620 (1927)
12. Bardeen J. and Shockley W., Phys. Rev. 80, 72 (1950)
13. Conwell E. and Weisskopf, V.F., Phys. Rev. 77, 388 (1950)
14. See for example Shockley, W., Electrons and Holes in Semiconductors p. 288, Van Nostrand Co. Princeton, (1950)
15. Moss, T.S., Optical Properties of Semiconductors p.155, Butterworths Scientific Publications, London 1959.
16. Kröger, F.A., Vink, H.J. and Volger, J., 1954, Physica 20, 1095
17. Piper W.W., and Halstead, R.E., 1960, Proceedings of the International Conference on Semiconductor Physics, Prague, 1047.
18. Collins, R.J., 1959, J. Appl. Phys. 30, 1135
19. Van Heerden, P.J. 1957, Phys. Rev. 106, 168.
20. Smith, R.W., 1957, Phys. Rev. 105, 900.
21. Hutson, A.R., McFee, J.H., White, D.L., 1961, Phys. Rev. letters, 237.

Administrative Details

Personnel: W.E. Spear ; J. Hart (Research Demonstrator at Leicester University)

Hours: W.E. Spear about 700 hrs.
J. Hart about 1500 hours.

Expenses: about 1000.